# 2D Imaging in Random Media with Active Sensor Array

## Paper Presentation: "Imaging and Time Reversal in Random Media"

Xianyi Zeng

**rhodusz@stanford.edu**

iCME, Stanford University

Math 221 Presentation
May 18 2010

# Outline


1. Random Medium Imaging: Super-Resolution and Self-Averaging
   - Mathematical Description of Inhomogeneous (Random) Medium
   - Time Reversal and Imaging in Random Media
2. Active Sensor Array: Cross-Range Resolution
   - Problem Setup
   - Modelling and SVD
   - DOA Estimation
3. Active Sensor Array: Range Resolution
   - Arrival Time Analysis
   - DOA with Arrival Times
   - Estimating Arrival Times
4. Subspace Arrival Time Analysis (SAT)

# Outline


1. Random Medium Imaging: Super-Resolution and Self-Averaging
   - Mathematical Description of Inhomogeneous (Random) Medium
   - Time Reversal and Imaging in Random Media
2. Active Sensor Array: Cross-Range Resolution
   - Problem Setup
   - Modelling and SVD
   - DOA Estimation
3. Active Sensor Array: Range Resolution
   - Arrival Time Analysis
   - DOA with Arrival Times
   - Estimating Arrival Times
4. Subspace Arrival Time Analysis (SAT)

# Outline

1. Random Medium Imaging: Super-Resolution and Self-Averaging
   - Mathematical Description of Inhomogeneous (Random) Medium
   - Time Reversal and Imaging in Random Media
2. Active Sensor Array: Cross-Range Resolution
   - Problem Setup
   - Modelling and SVD
   - DOA Estimation
3. Active Sensor Array: Range Resolution
   - Arrival Time Analysis
   - DOA with Arrival Times
   - Estimating Arrival Times
4. Subspace Arrival Time Analysis (SAT)

# Outline

1. Random Medium Imaging: Super-Resolution and Self-Averaging
   - Mathematical Description of Inhomogeneous (Random) Medium
   - Time Reversal and Imaging in Random Media
2. Active Sensor Array: Cross-Range Resolution
   - Problem Setup
   - Modelling and SVD
   - DOA Estimation
3. Active Sensor Array: Range Resolution
   - Arrival Time Analysis
   - DOA with Arrival Times
   - Estimating Arrival Times
4. Subspace Arrival Time Analysis (SAT)

**Wave equations and Green functions in random media:**

- Green function in time domain

$$\frac{1}{c(\mathbf{x})^2} G_{tt}(\mathbf{x}_0, \mathbf{x}, t) - \Delta_x G(\mathbf{x}_0, \mathbf{x}, t) = \delta(t)\delta(\mathbf{x}_0 - \mathbf{x})$$

- Green function in frequence domain

$$\left(\frac{\omega}{c(\mathbf{x})}\right)^2 \hat{G}(\mathbf{x}_0, \mathbf{x}, \omega) + \Delta_x \hat{G}(\mathbf{x}_0, \mathbf{x}, \omega) = -\delta(\mathbf{x}_0 - \mathbf{x})$$

- In homogeneous medium, $c(\mathbf{x}) \equiv c_0$, we have explicit expression for Green function:

$$\hat{G}_0(\mathbf{x}, \mathbf{y}, \omega) = \frac{\exp\left(ik|\mathbf{x} - \mathbf{y}|\right)}{4\pi|\mathbf{x} - \mathbf{y}|}$$

  here: $k = \omega / c_0$ is the wave number.

- In inhomogeneous medium, $\hat{G}(\mathbf{x}, \mathbf{y}, \omega)$ is not known, and can be very different from $\hat{G}_0(\mathbf{x}, \mathbf{u}, \omega)$:

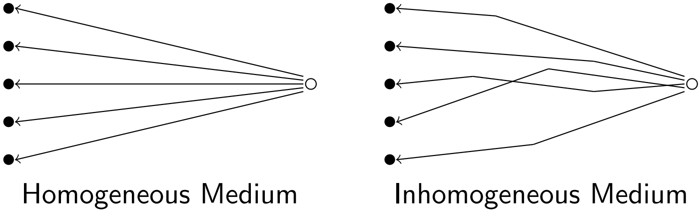


- The illuminating Green vector in homogeneous medium for a source $\mathbf{y}$ and N sensors $\mathbf{x}_p,\ p = 1, \ldots, N$ is known:

$$\hat{\mathbf{g}}_0(\mathbf{y}, \omega) = [\hat{G}_0(\mathbf{x}_1, \mathbf{y}, \omega), \ldots, \hat{G}_0(\mathbf{x}_N, \mathbf{y}, \omega)]^T$$

- The illuminating Green vector in inhomogeneous medium is not known:

$$\hat{\mathbf{g}}(\mathbf{y}, \omega) = [\hat{G}(\mathbf{x}_1, \mathbf{y}, \omega), \ldots, \hat{G}(\mathbf{x}_N, \mathbf{y}, \omega)]^T$$

**Time reversal in random media:**

- For simplicity, consider a passive sensor array given by $\mathbf{x}_p$, $1 \le p \le N$, and a source point $\mathbf{y}$ in random medium, emanating a short pulse $f(t)$. The recorded signal at $\mathbf{x}_p$ is:

$$\hat{\psi}(\mathbf{x}_p, \omega) = \hat{f}(\omega)\hat{G}(\mathbf{x}_p, \mathbf{y}, \omega)$$

- The physical time-reversed back-propogated field at a search point $\mathbf{y}^s$ is:

$$\begin{aligned}\hat{\Gamma}^{TR}(\mathbf{y}^s, \mathbf{y}, \omega) &= \sum_{p=1}^{N} \overline{\hat{\psi}(\mathbf{x}_p, \omega)}\hat{G}(\mathbf{x}_p, \mathbf{y}^s, \omega) \\ &= \overline{\hat{f}(\omega)} \sum_{p=1}^{N} \hat{G}(\mathbf{x}_p, \mathbf{y}^s, \omega)\overline{\hat{G}(\mathbf{x}_p, \mathbf{y}, \omega)}\end{aligned}$$

- $\Gamma^{TR}(\mathbf{y}^s, \mathbf{y}, t)$ is large when $\mathbf{y}^s$ is close to $\mathbf{y}$, and near $t = 0$.

**Self-averaging property of $\Gamma^{TR}(\mathbf{y}^s, \mathbf{y}, t)$:**

- Self-averaging: the recorded, time-reversed signals are sent back into the same random medium, hence phases of random Green functions $\hat{G}(\mathbf{x}_p, \mathbf{y}, \omega)$ and $\hat{G}(\mathbf{x}_p, \mathbf{y}^s, \omega)$ are approximately cancelled for each frequency $\omega$.
- Because of the self-averaging property, $\hat{\Gamma}^{TR}$ for different frequencies are statistically decorrelated:

$$E[\hat{\Gamma}^{TR}(\mathbf{y}^s, \mathbf{y}, \omega_1)\hat{\Gamma}^{TR}(\mathbf{y}^s, \mathbf{y}, \omega_2)] = E[\hat{\Gamma}^{TR}(\mathbf{y}^s, \mathbf{y}, \omega_1)]E[\hat{\Gamma}^{TR}(\mathbf{y}^s, \mathbf{y}, \omega_2)]$$

  for $\omega_1 \neq \omega_2$.
- Consequently, averaging over frequncies is like averaging over realizations of the random medium (for broad-band pulse):

$$\Gamma^{TR}(\mathbf{y}^s, \mathbf{y}, t) \approx E[\Gamma^{TR}(\mathbf{y}^s, \mathbf{y}, t)]$$

**Super-resolution property of $\Gamma^{TR}(\mathbf{y}^s, \mathbf{y}, t)$:**

- Super-resolution means, that for time reversal in random media, the cross-range resolution is better that the one in homogenous media, $\lambda L/a$.
- Super-resolution is a consequence of self-averaging property, that if the search point $\mathbf{y}^s$ is displaced from $\mathbf{y}$ by an amount $(\xi, 0)$, it can be calculated:

$$E[\overline{\hat{G}(\mathbf{x}_p, \mathbf{y}, \omega)}\hat{G}(\mathbf{x}_p, \mathbf{y}^s, \omega)] \approx \overline{\hat{G}_0(\mathbf{x}_p, \mathbf{y}, \omega)}\hat{G}_0(\mathbf{x}_p, \mathbf{y}^s, \omega) \exp\left(-\frac{k^2\xi^2 a_e^2}{2L^2}\right)$$

here $a_e = \sqrt{DL^3}$, where $D$ depends only on the statistics of the random fluctuations of $c(\mathbf{x})$.

- The multiplier is independent of $\mathbf{x}_p$:

$$\hat{\Gamma}^{TR}(\mathbf{y}^s, \mathbf{y}, \omega) = \hat{\Gamma}_0^{TR}(\mathbf{y}^s, \mathbf{y}, \omega) \exp\left(-\frac{k^2 \xi^2 a_e^2}{2L^2}\right)$$

- For search point off the target, fix $\xi > 0$, the back-propagated field in random medium has smaller amptitude than in homogeneous medium.
- At the target, $\xi \approx 0$, the back-propagated field in random medium has almost the same strength as in homogeneous medium.
- Super-resolution is obtained.

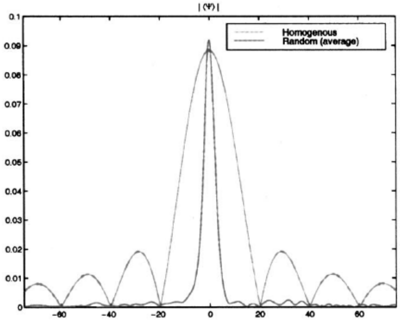


$L = 1000m$, $a = 50m$, average over 428 realizations for inhomogeneous case

**Imaging in random media**:

- For imaging, the recorded signals are back-propagated (analytically or numerically) in homogeneous medium, i.e. the imaging function is given by:

$$\hat{\Gamma}^{IM}(\mathbf{y}^s, \mathbf{y}, \omega) = \sum_{p=1}^{N} \overline{\hat{\psi}(\mathbf{x}_p, \omega)} \hat{G}_0(\mathbf{x}_p, \mathbf{y}^s, \omega)$$
$$= \overline{\hat{f}(\omega)} \sum_{p=1}^{N} \hat{G}_0(\mathbf{x}_p, \mathbf{y}^s, \omega) \overline{\hat{G}(\mathbf{x}_p, \mathbf{y}, \omega)}$$

- The deterministic Green function has no random phase, hence the random phases from the complex conjugate of random Green functions stays in imaging function $\hat{\Gamma}^{IM}$.

- $\hat{\Gamma}^{IM}$ is **not** self-averaging.
- We can not derive super-resolution property for imaging in random media, as we did for time reversal.
- Actually, $\Gamma^{IM}$ gives wider cross-range resolution than in homogeneous media.

- $\hat{\Gamma}^{IM}$ is **not** self-averaging.
- We can not derive super-resolution property for imaging in random media, as we did for time reversal.
- Actually, $\Gamma^{IM}$ gives wider cross-range resolution than in homogeneous media.

- $\hat{\Gamma}^{IM}$ is **not** self-averaging.
- We can not derive super-resolution property for imaging in random media, as we did for time reversal.
- Actually, $\Gamma^{IM}$ gives wider cross-range resolution than in homogeneous media.

## Conclusions:

- For locating targets in random media, estimators with self-averaging property are favored.
- Super-resolution is expected, when self-averaging property is satisfied.
- Self-averaging can be achieved, when any random Green function always appear in pair with a approximate complex conjugate random Green function (hence some time reversals are involved).
- For random media, self-averaging estimator should be used together with broad-band pulse, in order to give stable results. (Numerical examples shown later.)

**Problem setup:**

- Target: to image $M$ unknown scatterers with an active array of $N$ transducers in 2D plane. The number of scatters, i.e. $M$ is also unknown.

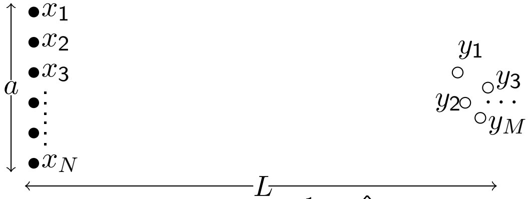


- Transducer spacing $h = a/(N-1) \approx \frac{1}{2}\lambda$; $\hat{f}(\omega)$ is the Fourier transform of probing pulse.
- The scatter $y_j,\ j = 1, \ldots, M$ are assumed to be sufficiently far apart, and they have scattering coefficients (reflectivity) $\hat{\rho}_j(\omega)$.

- Full data is assumed to be recorded: $\hat{P}(\omega) = [\hat{P}_{pq}(\omega)]$, $1 \leq p, q \leq N$.
- Questions:

1. How many objects are there?

$$M = ?$$

2. Where are they?

$$\mathbf{y}_j = ?\ j = 1, \ldots, M$$

- Full data is assumed to be recorded: $\hat{P}(\omega) = [\hat{P}_{pq}(\omega)]$, $1 \leq p, q \leq N$.
- Questions:
  1. How many objects are there?

$$M = ?$$

  2. Where are they?

$$\mathbf{y}_j = ?\ j = 1, \ldots, M$$

- Full data is assumed to be recorded: $\hat{P}(\omega) = [\hat{P}_{pq}(\omega)]$, $1 \leq p, q \leq N$.
- Questions:
  1. How many objects are there?

$$M = ?$$

  2. Where are they?

$$\mathbf{y}_j = ?\ j = 1, \ldots, M$$

**Point target model for response matrix**

- Let $\hat{G}$ be the Green function for random media as before. The pulse from $\mathbf{x}_q$, received by scatter $\mathbf{y}_j$ is $\hat{f}(\omega)\hat{G}(\mathbf{y}_j, \mathbf{x}_q, \omega)$. It will send back a reflected pulse: $\hat{\rho}_j(\omega)\hat{f}(\omega)\hat{G}(\mathbf{y}_j, \mathbf{x}_q, \omega)$.
- Neglecting any multiple scattering between unkown targets, the recorded signal at $\mathbf{x}_p$ from $\mathbf{x}_q$ will be:

$$\hat{\Pi}_{pq}(\omega) = \hat{f}(\omega) \sum_{j=1}^{M} \hat{\rho}_j(\omega)\hat{G}(\mathbf{y}_j, \mathbf{x}_p, \omega)\hat{G}(\mathbf{y}_j, \mathbf{x}_q, \omega)$$

- The full response matrix $\hat{\Pi}(\omega)$ in frequency domain should be:

$$\hat{P}(\omega) \approx \hat{\Pi}(\omega) = \hat{f}(\omega) \sum_{j=1}^{M} \hat{\rho}_j(\omega)\hat{\mathbf{g}}(\mathbf{y}_j, \omega)\hat{\mathbf{g}}(\mathbf{y}_j, \omega)^T$$

- Here $\hat{\mathbf{g}}(\mathbf{y}_j, \omega)$ is the illuminating Green vector onto the array from $\mathbf{y}_j$ in random media:

$$\hat{\mathbf{g}}(\mathbf{y}_j, \omega) = \begin{bmatrix} \hat{G}(\mathbf{y}_j, \mathbf{x}_1, \omega) \\ \hat{G}(\mathbf{y}_j, \mathbf{x}_2, \omega) \\ \vdots \\ \hat{G}(\mathbf{y}_j, \mathbf{x}_N, \omega) \end{bmatrix}$$

- For any $j$, $\hat{\mathbf{g}}(\mathbf{y}_j, \omega)^T \hat{\mathbf{g}}(\mathbf{y}_j, \omega)$ is a rank one matrix. Hence when $\mathbf{y}_j$ are far apart, $\hat{\Pi}(\omega)$ is a matrix with rank $M$.
- The rank of recorded data $\hat{P}(\omega) \approx \hat{\Pi}(\omega)$ has the rank equaling number of scatters:

$$\mathrm{rank}(\hat{P}) = M$$

**First application of SVD:**

- Calculate the SVD of the response matrix:

$$\hat{P}(\omega) = \hat{U}(\omega)\Sigma(\omega)\hat{V}^H(\omega)$$

  The diagonal matrix $\Sigma(\omega)$ has non-negative diagonal elements:

$$\sigma_1(\omega) \geq \sigma_2(\omega) \geq \cdots \geq \sigma_{M'}(\omega) > \sigma_{M'+1}(\omega) \approx \cdots \approx \sigma_N(\omega) \approx 0$$

- Columns of $\hat{U}(\omega)$: $\hat{U}_r(\omega)$ is the left singular vector associated with $\sigma_r(\omega)$; and it's also the eigenvector of $\hat{P}(\omega)\hat{P}(\omega)^H$ associated with the eigenvalue $\sigma_r^2(\omega)$.
- The rank of response data $\hat{P}(\omega)$ is approximately $M'$, the rank of diagonal matrix $\Sigma$.

# Active Sensor Array: Cross-Range Resolution
## Modelling and SVD

- We must have: $M \approx M'$, and for media with small fluctuation; $M = M'$, for any frequency $\omega$ within bandwidth of probing pulse.
- Some examples of two targets in both homogeneous and inhomogeneous medium:

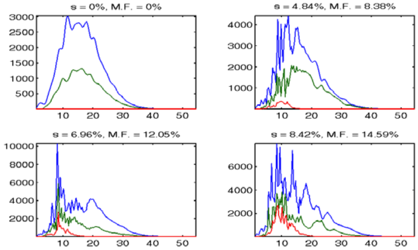


First three singular values from simulations with two targets in the medium

**Information about singular vectors:**

- Targets are far apart, thus $\hat{\mathbf{g}}(\mathbf{y}_j, \omega)$ are approximately orthogonal to each other.
- Left singular vectors $\hat{U}_r(\omega),\ 1 \leq r \leq M$ are calculated from SVD of $\hat{P}(\omega)$, from the modelling, they should be:

$$\hat{U}_r(\omega) \approx e^{i\phi(\omega)} \frac{\hat{\mathbf{g}}(\mathbf{y}_j, \omega)}{|\hat{\mathbf{g}}(\mathbf{y}_j, \omega)|}$$

$$\sigma_r(\omega) \approx |\hat{f}(\omega)||\hat{\rho}_j(\omega)||\hat{\mathbf{g}}(\mathbf{y}_j, \omega)|^2$$

Here $\phi(\omega)$ is an arbitrary phase, depending on the algorithm used to performing the SVD.

**Try beam-forming:**

- Beam-forming takes inner product of singular vector with normalized illumination vector.
- In random media case, $\hat{\mathbf{g}}(\mathbf{y}^s, \omega)$ is unknown. Hence the known illumination vector in homogeneous medium, $\hat{\mathbf{g}}_0(\mathbf{y}^s, \omega)$ is tried:

$$\hat{U}_r^H(\omega)\frac{\hat{\mathbf{g}}_0(\mathbf{y}^s,\omega)}{|\hat{\mathbf{g}}_0(\mathbf{y}^s,\omega)|} \approx e^{i\phi(\omega)}\frac{\hat{\mathbf{g}}(\mathbf{y}_j,\omega)^H\hat{\mathbf{g}}_0(\mathbf{y}^s,\omega)}{|\hat{\mathbf{g}}(\mathbf{y}_j,\omega)||\hat{\mathbf{g}}_0(\mathbf{y}^s,\omega)|}$$

- Difficulty 1: unknown phase $\phi(\omega)$. It can be fixed by computing singular vectors using power method.
- Difficulty 2: random Green function is not compensated by a complex conjugate one which cancels the large random phases, hence not self-averaging.

**Statistically stable broad-band DOA estimation:**

- $\hat{P}(\omega)\hat{P}^H(\omega)$ is known, and it provides random Green function and complex conjugate of random Green function naturally:

$$\left[\hat{P}(\omega)\hat{P}^H(\omega)\right]_{pq} = \sum_{r=1}^{N} \hat{P}_{pr}(\omega)\overline{\hat{P}_{rq}(\omega)} \approx \sum_{r=1}^{N} \hat{\Pi}_{pr}(\omega)\overline{\hat{\Pi}_{rq}(\omega)}$$

- Apply MUSIC (multiple signal classification): looking for $\mathbf{y}^s$ whose illumitating Green vector is orthogonal to null space of $\hat{P}(\omega)\hat{P}^H(\omega)$.
- Observation: if the random vector $\hat{\mathbf{g}}(\mathbf{y}^s, \omega)$ is orthogonal to the null space of $\hat{\Pi}(\omega)\hat{\Pi}^H(\omega) \approx \hat{P}(\omega)\hat{P}^H(\omega)$, then $\mathbf{y}^s$ must coincide with one of $\mathbf{y}_j$, for some $1 \leq j \leq M$.

- We cannot project $\hat{\mathbf{g}}(\mathbf{y}^s, \omega)$, since it is unknown; instead, the deterministic illuminating vector $\hat{\mathbf{g}}_0(\mathbf{y}^s, \omega)$ is projected to the null space of $\hat{P}(\omega)\hat{P}^H(\omega)$:

$$\mathcal{P}_N \hat{\mathbf{g}}_0(\mathbf{y}^s, \omega) = \sum_{r=1}^{M} \left[\hat{U}_r^H(\omega)\hat{\mathbf{g}}_0(\mathbf{y}^s, \omega)\right] \hat{U}_r(\omega) - \hat{\mathbf{g}}_0(\mathbf{y}^s, \omega)$$

- If $\hat{P}(\omega) = \hat{\Pi}(\omega)$, and the random illuminating vector comes from a target $\mathbf{y}_j$, the projection nearly zero:

$$\mathcal{P}_N \hat{\mathbf{g}}(\mathbf{y}_j, \omega) \approx \left[\hat{U}_j^H(\omega)\hat{\mathbf{g}}(\mathbf{y}_j, \omega)\right] \hat{U}_j(\omega) - \hat{\mathbf{g}}(\mathbf{y}_j, \omega) = 0$$

# Active Sensor Array: Cross-Range Resolution
## DOA Estimation

- Normalize the projection by singular value $\sigma_j(\omega)$:

$$\hat{\mathcal{F}}^{(j)}(\mathbf{y}^s, \omega) = \sigma_j(\omega)\mathcal{P}_N \hat{\mathbf{g}}_0(\mathbf{y}^s, \omega)$$

- Apply the inverse Fourier transform (up to a constant):

$$\mathcal{F}^{(j)}(\mathbf{y}^s, t) = \int e^{-i\omega t}\sigma_j(\omega)\sum_{r=1}^{M}\left[\hat{U}_r^H(\omega)\hat{\mathbf{g}}_0(\mathbf{y}^s, \omega)\hat{U}_r(\omega)d\omega\right] - \int e^{-i\omega t}\sigma_j(\omega)\hat{\mathbf{g}}_0(\mathbf{y}^s, \omega)d\omega$$

- The second term of $\mathcal{F}_p^{(j)}(\mathbf{y}^s, t)$ has deterministic arrival time: $t_p(\mathbf{y}^s) = |\mathbf{x}_p - \mathbf{y}^s|/c_0$.
- The second term of $\mathcal{F}_p^{(j)}(\mathbf{y}^s, t_p(\mathbf{y}^s))$ resembles $f(0) \approx 0$ up to a constant.

# Active Sensor Array: Cross-Range Resolution
## DOA Estimation

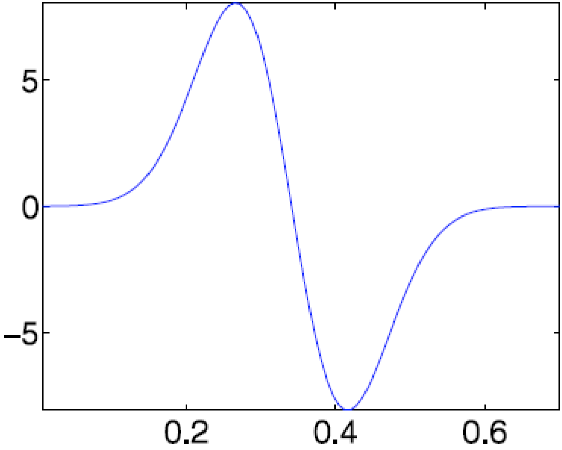


Probing pulse $f(t)$

- Define the sum:

$$\mathcal{G}^{(j)}(\mathbf{y}^s) = \sum_{p=1}^{N} \left( \mathcal{F}_p^{(j)}(\mathbf{y}^s, t_p(\mathbf{y}^s)) \right)^2 \tag{1}$$

- When $\mathbf{y}^s \approx \mathbf{y}_j$, $\mathcal{P}_N \hat{\mathbf{g}}_0(\mathbf{y}^s, \omega) \approx \mathcal{P}_N \hat{\mathbf{g}}(\mathbf{y}^s, \omega) \approx 0$, hence for any $t$, $\mathcal{F}^{(j)}(\mathbf{y}^s, t) \approx \mathbf{0}$, thus $\mathcal{G}^{(j)}(\mathbf{y}^s) \approx 0$.
- The objective functional defined as:

$$\mathcal{R}(\mathbf{y}^s) = \sum_{j=1}^{M} \frac{\min_{\mathbf{y}} \mathcal{G}^{(j)}(\mathbf{y})}{\mathcal{G}^{(j)}(\mathbf{y}^s)} \tag{2}$$

should has peak values near $\mathbf{y}_j$, $1 \leq j \leq M$, since one of the denominators is nearly zero.

**Claim: the estimator is self-averaging**:

- This can be illustrated both mathematically and physically for one target case ($M = 1$).
- When there is only one target:

$$\mathcal{F}(\mathbf{y}^s, t) = \mathcal{B}(\mathbf{y}^s, t) - \mathcal{A}(\mathbf{y}^s, t)$$

with

$$\hat{\mathcal{A}}(\mathbf{y}^s, \omega) = |\hat{f}(\omega)||\hat{\rho}(\omega)|\hat{\mathbf{g}}_0(\mathbf{y}^s, \omega) \sum_{p=1}^{N} \hat{G}(\mathbf{y}_1, \mathbf{x}_p, \omega)\overline{\hat{G}(\mathbf{y}_1, \mathbf{x}_p, \omega)}$$

$$\hat{\mathcal{B}}(\mathbf{y}^s, \omega) = |\hat{f}(\omega)||\hat{\rho}(\omega)|\hat{\mathbf{g}}(\mathbf{y}_1, \omega) \sum_{p=1}^{N} \hat{G}_0(\mathbf{y}^s, \mathbf{x}_p, \omega)\overline{\hat{G}(\mathbf{y}_1, \mathbf{x}_p, \omega)}$$

- Clearly $\hat{\mathcal{A}}(\mathbf{y}^s, \omega)$ is self-averaging.
- The $q$-th component of $\hat{\mathcal{B}}(\mathbf{y})^s, \omega$ is:

$$\hat{\mathcal{B}}_q(\mathbf{y}^s, \omega) = |\hat{f}(\omega)||\hat{\rho}(\omega)| \sum_{p=1}^{N} \hat{G}_0(\mathbf{y}^s, \mathbf{x}_p, \omega) \hat{G}(\mathbf{y}_1, \mathbf{x}_q, \omega) \overline{\hat{G}(\mathbf{y}_1, \mathbf{x}_p, \omega)}$$

  Random Green functions are compensated for approximation of its complex conjugate random Green function.
  Hence $\hat{\mathcal{B}}(\mathbf{y}^s, \omega)$ is also self-averaging.
- The explanations can be given physically, in terms of time-reversal.

**Comparison between broad-band simulation and single-frequency simulation:**

- Methods using (2) with a broad-band pulse, and a single-frequency pulse are simulated, to imaging one or two targets in homogeneous or random media:

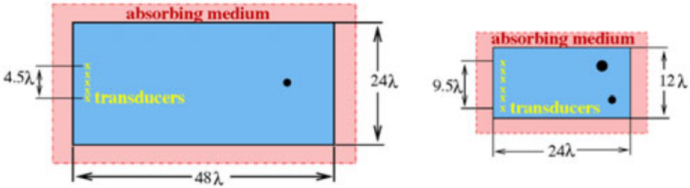


Problem setups for one-target case and two-target case.

- Imaging one target:

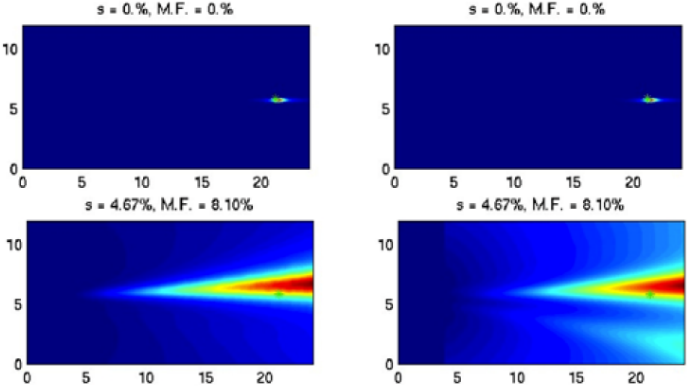


Left: broad-band. Right: single-frequency.

- Imaging two targets:

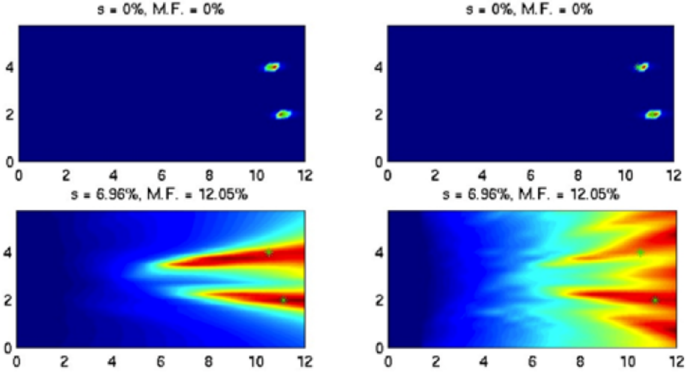


Left: broad-band. Right: single-frequency.

## Conclusions:

- Beam-forming method is not self-averaging, hence not adviced.
- A method based on MUSIC is proposed for imaging, which is shown to be self-averaging.
- Statistical stable results can be obtained by using broad-band probing pulse.
- The DOA estimator $\mathcal{R}(\mathbf{y}^s)$ gives good cross-range resolution, but bad range resolution.

**Why no range-resolution?**

- Object functional (2) gives reasonable cross-range resolution; however the range resolution is not good at all.
- The reason is that we use the arrival time $t_p(\mathbf{y}^s)$ (which is the arrival time for $\mathcal{A}(\mathbf{y}^s, t)$) as a crude estimation for that of the whole function $\mathcal{F}(\mathbf{y}^s, t)$ in (1).
- Suppose $\tau_p^{(j)}$ is an estimation to the exact travel time between $\mathbf{x}_p$ and $\mathbf{y}_j$ in the random medium.
- Assuming one target, due to self-averaging property of $\mathcal{F}_q^{(1)}(\mathbf{y}^s, t)$, we can approximate the product $\overline{\hat{G}(\mathbf{y}_1, \mathbf{x}_p, \omega)}\hat{G}(\mathbf{y}_1, \mathbf{x}_q, \omega)$ by its expectation:

- Define $r_p = |\mathbf{x}_p - \mathbf{y}_1|$, $r_p^s = |\mathbf{x}_p - \mathbf{y}^s|$.

$$E[\overline{\hat{G}(\mathbf{y}_1, \mathbf{x}_p, \omega)}\hat{G}(\mathbf{y}_1, \mathbf{x}_q, \omega)] \approx \frac{e^{-\beta(\omega)|\mathbf{x}_p - \mathbf{x}_q|^2}}{(4\pi)^2 r_p r_q} e^{-i\omega(\tau_p^{(1)} - \tau_q^{(1)})}$$

- To illustrate the sensitivity of $\mathcal{F}$ on traveling time, test simulations are setup, assuming $|\hat{\rho}(\omega)| = 1$, $\beta(\omega) \equiv \beta$, and replace $|\hat{f}(\omega)|$ with $\hat{f}(\omega)$, $\mathcal{F}_q^{(1)}(\mathbf{y}^s, t)$ is approximated by:

$$\begin{aligned} \mathcal{M}_q(\mathbf{y}^s, t) = \ & \tfrac{1}{(4\pi)^2} \textstyle\sum_{p=1}^N \left\{ \tfrac{e^{-\beta|\mathbf{x}_p - \mathbf{x}_q|^2}}{r_p r_q r_p^s} f(t + \tau_p^{(1)} - \tau_q^{(1)} - t_p(\mathbf{y}^s)) \right. \\ & \left. - \tfrac{1}{r_p^2 r_q^s} f(t - t_q(\mathbf{y}^s)) \right\} \end{aligned} \tag{3}$$

- Using $\mathcal{M}_q(\mathbf{y}^s, t)$ instead of $\mathcal{F}_q^{(1)}(\mathbf{y}^s, t)$ in (2), the results are almost reproduced:

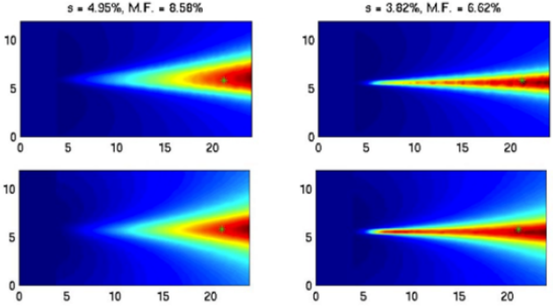


Top: using $\mathcal{F}$; bottom: using $\mathcal{M}$

- Here estimations $\tau_p^{(1)} = \tau_{p,DG}^{(1)}$ based on diagonal of $\hat{P}(\omega)$ are used.

# Active Sensor Array: Range Resolution
## Arrival Time Analysis

- We can look at (3) for answering why there is no range-resolution by using (2) with (1).
- Using $t = t_q(\mathbf{y}^s)$ only minimize the second term in $\mathcal{M}_q(\mathbf{y}^s, t)$, the first term has a differential arriving time:

$$t_q(\mathbf{y}^s) + \tau_p^{(1)} - \tau_q^{(1)} - t_p(\mathbf{y}^s)$$

- It is the difference between travel times in random medium that plays an important role in imaging, not the travel time.
- There is essentially no range information in $\mathcal{M}$, hence $\mathcal{F}$ cannot give good range-resolution.

**Improvement: choosing different $t$ for $\mathcal{B}$:**

- If we choose $t = \tau_q^{(1)}$ for first term in (3), the value of $\mathcal{M}$ will depends on travel time directly:

$$\tau_q^{(1)} + \tau_p^{(1)} - \tau_q^{(1)} - t_p(\mathbf{y}^s) = \tau_p^{(1)} - t_p(\mathbf{y}^s)$$

- This suggests the estimator using:

$$\mathcal{H}_q^{(1)}(\mathbf{y}^s) = \mathcal{B}_q^{(1)}(\mathbf{y}^s, \tau_q^{(1)}) - \mathcal{A}_q^{(1)}(\mathbf{y}^s, t_q(\mathbf{y}^s)) \tag{4}$$

$$\mathcal{G}_\tau^{(1)}(\mathbf{y}^s) = \sum_{p=1}^{N} (\mathcal{H}_p^{(1)}(\mathbf{y}^s))^2$$

- Imaging is to maximizing the **DOA-AT** estimator:

$$\mathcal{R}_\tau(\mathbf{y}^s) = \frac{\min_{\mathbf{y}} \mathcal{G}_\tau^{(1)}(\mathbf{y})}{\mathcal{G}_\tau^{(1)}(\mathbf{y}^s)} \tag{5}$$

- By using an estimator $\tau^{(1)}_{p,SVD}$ based on SVD of $\hat{P}(\omega)$, the imagings of previous examples:

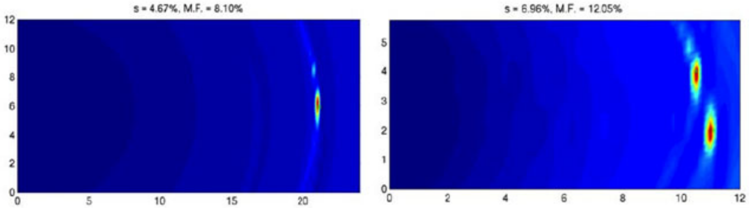


- Both cross-range and range resolutions are good.
- However, the usefulness of estimator (5) relies on a good travel time estimator.

**Using diagonal of response matrix to estimate arrival times:**

- If one keep track of $P_{pp}(t)$, the arrival times of pulses will be twice the travel time between $\mathbf{x}_p$ and targets.
- The signals are clean in homogeneous medium:

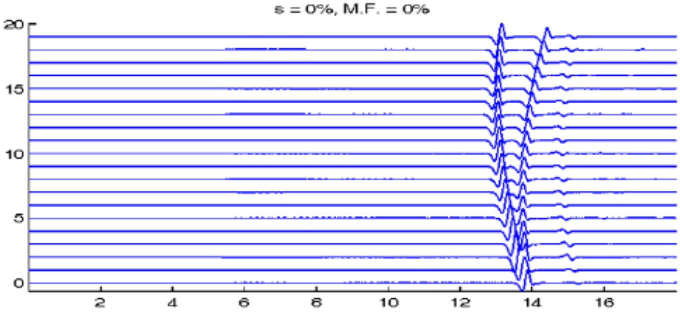


Two peaks are clearly distinguished in homogeneous medium

- In random medium, the signals are not so clean:

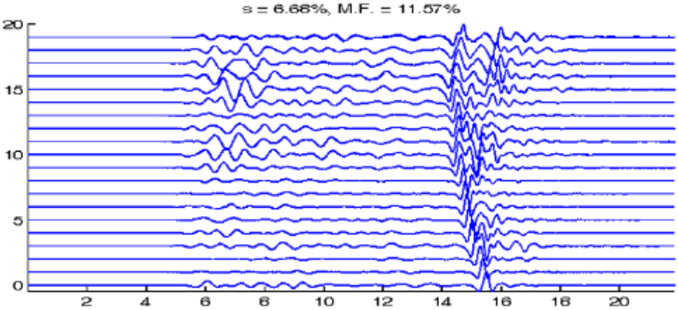


Scattered fronts from two targets are difficult to interpret in random medium

- Let $\tau_{p,DG}^{(j)}$ be the estimated arrival times for $j$-th scattered front.
- ATA estimator functional:

$$\mathcal{G}_{ATA}^{(j)}(\mathbf{y}^s) = \sum_{p=1}^{N} \left[\tau_{p,DG}^{(j)} - 2t_p(\mathbf{y}^s)\right]^2$$

Imaging is to maximize:

$$\mathcal{R}_{ATA}(\mathbf{y}^s) = \sum_{j=1}^{M} \frac{\min_{\mathbf{y}} \mathcal{G}_{ATA}^{(j)}(\mathbf{y})}{\mathcal{G}_{ATA}^{(j)}(\mathbf{y}^s)}$$

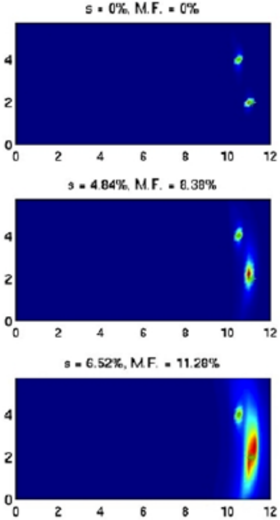

**Using singular vectors from SVD to estimate arrival times:**

- The idea is that the trace of the singular vector $U_r(t)$ have only one front (arrival time) back-scattered by the target that makes the largest contribution to $\sigma_j(\omega)$.
- Assumption: contribution of some Green vector $\hat{\mathbf{g}}(\mathbf{y}_j, \omega)$ in $\hat{U}_r(\omega)$ is more significant than that of $\hat{\mathbf{g}}(\mathbf{y}_h, \omega)$ for all $h \neq j$.
- Suppose $\mathbf{y}_1$ is the strongest target associated with $\sigma_1(\omega)$. Difficulty: $\hat{U}_1(\omega)$ has an unknown, arbitrary, frequency dependent phase. Hence $U_1(t)$ looks incoherent in time domain.
- We can project columns of $\hat{P}(\omega)$ onto the singular vector $\hat{U}_1(\omega)$ to remove the unknown phase:

$$\hat{U}_1^{(p)}(\omega) = \left[\hat{U}_1(\omega)^H \hat{P}^{(p)}(\omega)\right] \hat{U}_1(\omega) \quad p = 1, \ldots, N$$

- For different $\mathbf{x}_p$, the arrival times are different (introduced by different Green functions $\hat{G}(\mathbf{x}_p, \mathbf{y}_1, \omega)$).
- They can be synchronized and then be averaged to obtain the effective singular vector:

$$U_1(t) = \frac{1}{N} \sum_{p=1}^{N} U_1^{(p)}(t - \tau_p^{(1)})$$

- Here $\tau_p^{(1)}$ are estimated as the minimizer of integrated squared error:

$$\min_{\tau_p^{(1)}} \int_0^T \sum_{p=1}^{N} \left[ U_1^{(p)}(t - \tau_p^{(1)}) - U_1(t) \right]^2 dt$$

- Comparison of matrix diagonals and averaged singular vector in homogeneous medium:

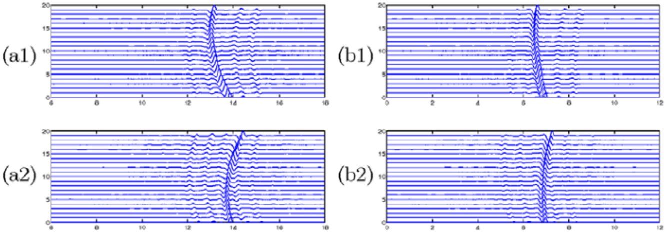


- The results are essentially the same.

- Comparison of matrix diagonals and averaged singular vector in inhomogeneous medium:

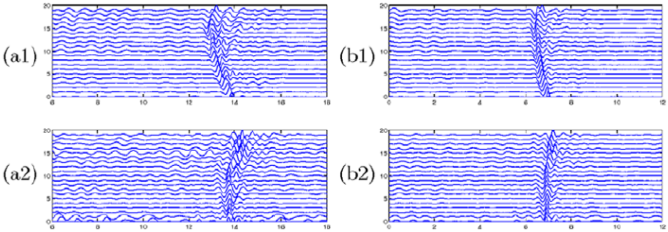


- Much cleaner fronts are obtained by using averaged sinvular vectors.

## Conclusions:

- Estimator $\mathcal{R}(\mathbf{y}^s)$ has poor range resolution because it depends on differential arrival times rather than arrival times.
- Estimator $\mathcal{R}_\tau(\mathbf{y}^s)$, using different times for $\mathcal{B}$ and $\mathcal{A}$, can have both good cross-range resolution and reasonable range resolution. But they may be sensitive to the choice of arrival time estimator.
- One can use only the arrival time estimation to obtain good range resolution, like $\mathcal{R}_{ATA}(\mathbf{y}^s)$.
- For random medium, arrival time estimator based on SVD is better than estimator based on diagonals of response matrix.

# SAT

**An estimator combines both DOA analysis and ATA:**

- Minimizers for $[\mathcal{F}_p^{(j)}(\mathbf{y}^s, t_p(\mathbf{y}^s))]^2$ gives good cross-range resolution.
- Minimizers for $[\tau_{p,SVD}^{(j)} - t_p(\mathbf{y}^s)]^s$ gives good range resolution.
- SAT estimator combines the two, and define:

$$\mathcal{G}_{SAT}^{(j)}(\mathbf{y}^s) = \sum_{p=1}^{N} \left[\mathcal{F}_p^{(j)}(\mathbf{y}^s, t_p(\mathbf{y}^s))\right]^2 \left[\tau_{p,SVD}^{(j)} - t_p(\mathbf{y}^s)\right]^2$$

- The objective functional to be maximized:

$$\mathcal{R}_{SAT}(\mathbf{y}^s) = \sum_{j=1}^{M} \frac{\min_{\mathbf{y}} \mathcal{G}_{SAT}^{(j)}(\mathbf{y})}{\mathcal{G}_{SAT}^{(j)}(\mathbf{y}^s)}$$

# SAT

- Imaging one target using SAT:

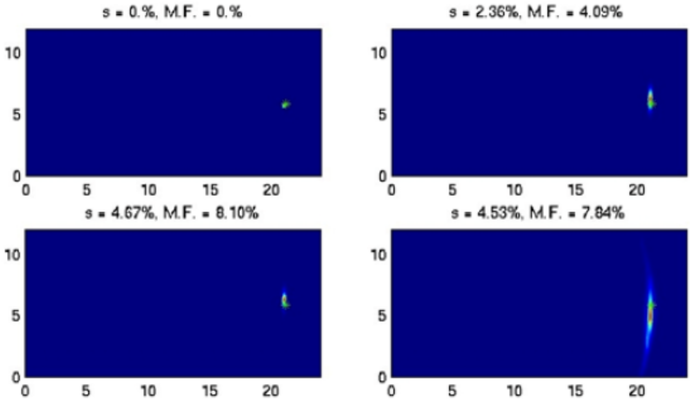

# SAT

- Imaging two targets using SAT:

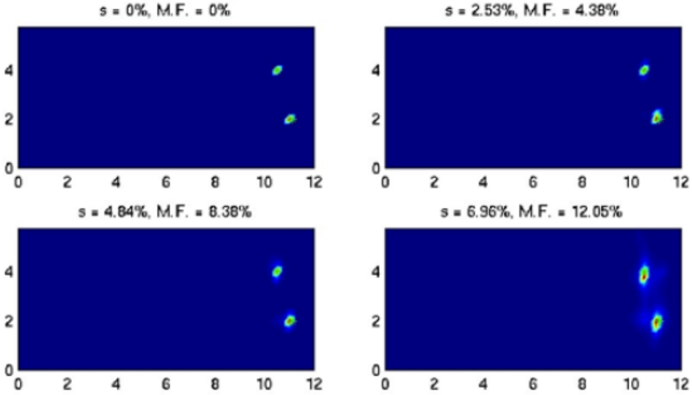

# SAT

## Conclusions:

- $\mathcal{R}_{SAT}$ can give both good cross-range resolution (it is self-averaging) and good range resolution (there is arrival time estimation).
- $\mathcal{R}_{SAT}$ is robust, in the sense that the dependency on arrival time estimator is decreased by multiplication with $\mathcal{F}_p^{(j)}$, which is independent of arrival time estimation.

## Materials not covered:

- SAI (synthetic aperture imaging) estimators, which only use diagonals of $\hat{P}(\omega)$. The estimator gives good range resolution but poor cross-range resolution, since it is not self-averaging.
- Use SAI estimator to improve range resolution of $\mathcal{R}(\mathbf{y}^s)$.
- Analysis of multiple scattering between targets (complication of modelling).

# SAT

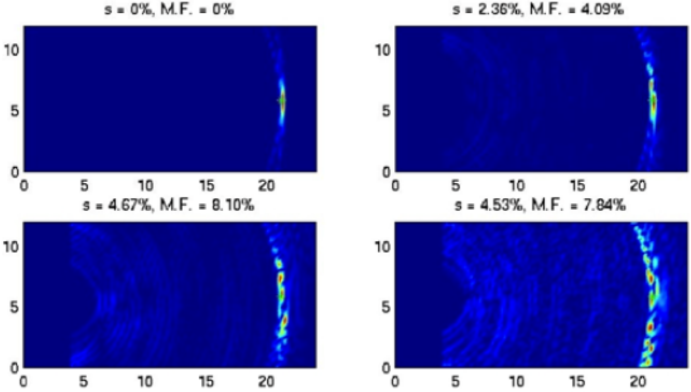


Imaging using SAI estimator, an example of non-self-averaging estimators.

# References


P. Blomgren, G. Papanicolaou, and H. Zhao.
Super-resolution in time-reversal acoustics.
*Journal of Acoustical Society of America*, 111:238–248, 2002.

L. Borcea, G. Papanicolaou, and C. Tsogka.
Theory and applications of time reversal and interferometric imaging.
*Inverse Problems*, 19:S139–S164, 2003.

L. Borcea, G. Papanicolaou, C. Tsogka, and J. Berryman.
Imaging and time reversal in random media.
*Inverse Problems*, 18:1247–1279, 2002.

R. O. Schmidt.
Multiple emitter location and signal parameter estimation.
*IEEE Transactions on Antennas and Propagation*, 34:276–280, 1986.